



Synthesis and characterization of nanocrystalline PZT powders: From sol to dense ceramics

Ali Mirzaei^{1,*}, Maryam Bonyani¹, Shahab Torkian²

¹Department of Materials Science and Engineering, Shiraz University, Shiraz, Iran

²Materials Engineering Department, Malek Ashtar University of Technology, Shahin Shahr, Iran

Received 26 December 2015; Received in revised form 5 February 2016; Accepted 18 February 2016

Abstract

In this study ferroelectric lead zirconate titanate PZT (0.523/0.477) nanocrystalline powders have been successfully synthesized by an alkoxide based sol-gel process. Crystallinity of the prepared ceramic powders was studied using X-ray diffractometer. Scanning electron microscopy (SEM) and transmission electron microscopy (TEM) studies were performed to study morphology of the calcined powders. EDX analysis was employed to demonstrate purity of the synthesized powders. Surface nature of the powders was studied by using FTIR technique. TGA/DTA analysis was employed to study thermal behaviour of powders. Spectroscopic techniques (FTIR and XRD) results indicated that the as-dried amorphous powders can be completely crystallized at 600 °C. In order to investigate the densification behaviour of the calcined powders, the crystalline PZT powders were pelletized into discs and sintered at various temperatures from 900 °C to 1150 °C, with a heating rate of 10 °C/min and holding time of 2 h to find the optimum combination of temperature and time to produce high density ceramics. Microstructural characterization was conducted on the fractured surface of the samples using SEM. It was found that the PZT ceramics calcined at 600 °C for 4 h then sintered at 1050 °C for 2 h had maximal density (98% of the theoretically density).

Keywords: ferroelectric, PZT, sol-gel process, XRD, FTIR, sintering

I. Introduction

Lead zirconate titanate ($\text{Pb}(\text{Zr}_{1-x}\text{Ti}_x)\text{O}_3$, PZT) having a perovskite type ABO_3 structure is a solid solution of a ferroelectric phase i.e. lead titanate (PbTiO_3) and an antiferroelectric phase, i.e. lead zirconate (PbZrO_3) [1]. In the 1950's, Jaffe *et al.* discovered that PZT ceramics with a Zr/Ti ratio approximately 52:48 have excellent properties such as, high Curie temperature, high electromechanical coupling coefficient, easy poling and doping, and high dielectric, ferroelectric and piezoelectric properties. Owing to these excellent properties, PZT ceramics have been extensively used in many applications such as nonvolatile ferroelectric random access memories (NVRAMs), pressure and force sensors, accelerometer, microphones, air and underwater transducers, FM coupled mode filters, actuators, etc. [3,4]. Traditionally PZT ceramics are prepared by solid-state reaction process because of their facile processing and eco-

nomic considerations [5]. In this process mechanically mixed starting materials, which are typically oxides or carbonates, are heated at high temperatures to obtain desired product [6]. However, high calcinations temperatures employed in this method lead to aggregation of powders and loss of PbO which are responsible for degradation of electrical properties of PZT ceramics [7]. Furthermore, low homogeneity due to poor mixing and low purity due to presence of impurities in raw materials and contaminations from jar are other drawbacks of solid-state process [8,9]. Accordingly, in order to obtain PZT ceramics with good electrical properties, it is necessary to use other methods for synthesis of fine and homogeneous PZT powders with high purity. For synthesis of such powders, in recent years chemical methods such as sol-gel [10,11], citrate nitrate [12], hydrothermal [13], spray drying [14], co-precipitation [15], sol-hydrothermal [16] etc., were used. Owing to mixing of components at molecular level and purity of starting materials, all of these methods result in fine, homogeneous and pure powders. However, among these methods, sol-

* Corresponding author: tel: +98 71 3721 1984, fax: +98 71 3721 1984, e-mail: alisonmirzaee@yahoo.com

gel method has been widely employed for synthesis of PZT powders. This is due to inherent advantages of this process, such as simple set up, high homogeneity, high purity and excellent control of stoichiometry [17,18]. Besides, the use of highly reactive metal alkoxides as precursors allows the synthesis of ceramic materials at lower temperatures than other common solid state reactions [19]. Finally, the rheological properties of sols or gels of this technique provide a new approach to the preparation of powders, thin films [20], fibers [21] and porous ceramics [22].

The present work concerns the synthesis of PZT nanocrystalline powders via sol-gel method with a special attention to characterization of synthesized powders from sol to dense ceramics. Also sintering behaviour of dense ceramics was studied.

II. Experimental procedure

2.1. Nanocrystalline PZT powder preparation

The starting chemical materials were lead (II) acetate trihydrate, ($\text{Pb}[\text{CH}_3\text{COO}]_2 \times 3 \text{H}_2\text{O}$), (99.5%, Merck), zirconium (IV) n-propoxide, ($\text{Zr}[\text{OCH}(\text{CH}_3)_2]_4$), (70% w/w in n-propanol, Fluka) and titanium (IV) isopropoxide, ($\text{Ti}[\text{OCH}(\text{CH}_3)_2]_4$), (99% Merck). 2-methoxy ethanol ($\text{CH}_3\text{O}(\text{CH}_2)_2\text{OH}$) (99.5%, Merck) was used as solvent and acetylacetone ($\text{C}_5\text{O}_5\text{H}_8$, AcAc), (99.9%, Merck) was used as a stabilizer for alkoxides. To produce 200 ml, 0.5 M PZT (52/48) sol, 41.73 g (slightly higher than stoichiometry amount, to compensate the loss of lead in the subsequent thermal treatment) lead acetate trihydrate was dissolved in 80 ml, 2-methoxyethanol while stirred at 120 °C for 2 hours and then refluxed at the same temperature for another 2 hours in order to obtain a homogeneous solution. The by-products of this solution were vacuum distilled in 80 °C until a white paste (i.e. the Pb precursor paste) was formed. In a separate flux stoichiometric amounts of titanium (IV) isopropoxide (13.344 g) and zirconium (IV) n-propoxide (23.308 g) were dissolved in 40 ml 2-methoxyethanol in presence of 10.012 g acetylacetone (the molar ratio was $[\text{Zr}+\text{Ti}]/[\text{AcAc}]=1/1$) at ambient temperature. Then the solution was refluxed at 120 °C for 2 hours forming a clear yellow solution (i.e. the

Ti/Zr precursor solution). The next step was mixing of the Pb paste and Ti/Zr solution and formation of a new solution, which was refluxed at 120 °C for 3 hours. Then hydrolyzing agent (distilled water in molar ratio $[\text{Ti}]/[\text{H}_2\text{O}] = 1/2$) was added to the solution and refluxed at 120 °C for another 1 hour. The final product was a viscous golden solution so called “PZT sol” (Fig. 1a). The PZT concentration on the final sol was 0.5 M with pH ~ 7 . The PZT sol was converted to a gel at 80 °C for 4 h and after drying at 120 °C for 24 h the gel was transformed to amorphous powder. The obtained amorphous powders were heat treated at 600–700 °C for different times to obtain crystalline PZT powders.

2.2. Preparation of PZT ceramics

The crystalline PZT powders were used for preparation of PZT discs. The PZT powders were mixed with 5 wt.% of a water solution containing 10% polyvinyl alcohol (PVA). The powders were pressed into 10 mm in diameter by 1.5 mm thick discs in stainless steel dies under uniaxial pressure at 150 MPa. Then the samples were placed in a covered alumina crucible and atmosphere was controlled by the addition of pure PZT (52/48) + 10% ZnO powders in the crucible without contact with the samples (Fig. 1b). The discs were sintered at various temperatures from 900–1150 °C for 2 h, with 4 h holding at 550 °C for binder burn-out of organic species. Heating rate was 5 °C/min up to burn-out temperature (550 °C) and then a heating rate of 10 °C/min was employed up to final sintering temperature. Figure 2 shows the detailed scheme of the experimental procedure.

2.3. Characterization

The phase composition of the powders and sintered bodies was examined by X-ray diffractometer (Bruker-Germany) using $\text{CuK}\alpha$ radiation ($\lambda = 1.5418 \text{ \AA}$). The XRD patterns were recorded at room temperature at a scan rate 0.05°/s and 2θ from 20° to 70°. Microstructural characterization was conducted by fractured surface of sintered samples using scanning electron microscopy (SEM- Cambridge). The density of sintered samples was determined by the Archimedes method. Particle size analysis of synthesized powders was per-

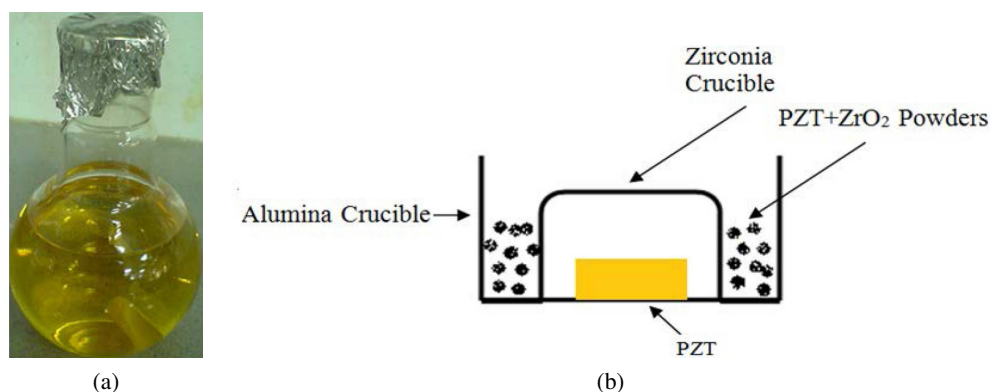


Figure 1. PZT sol (a) and schematic representation of set-up used for sintering of PZT discs (b)

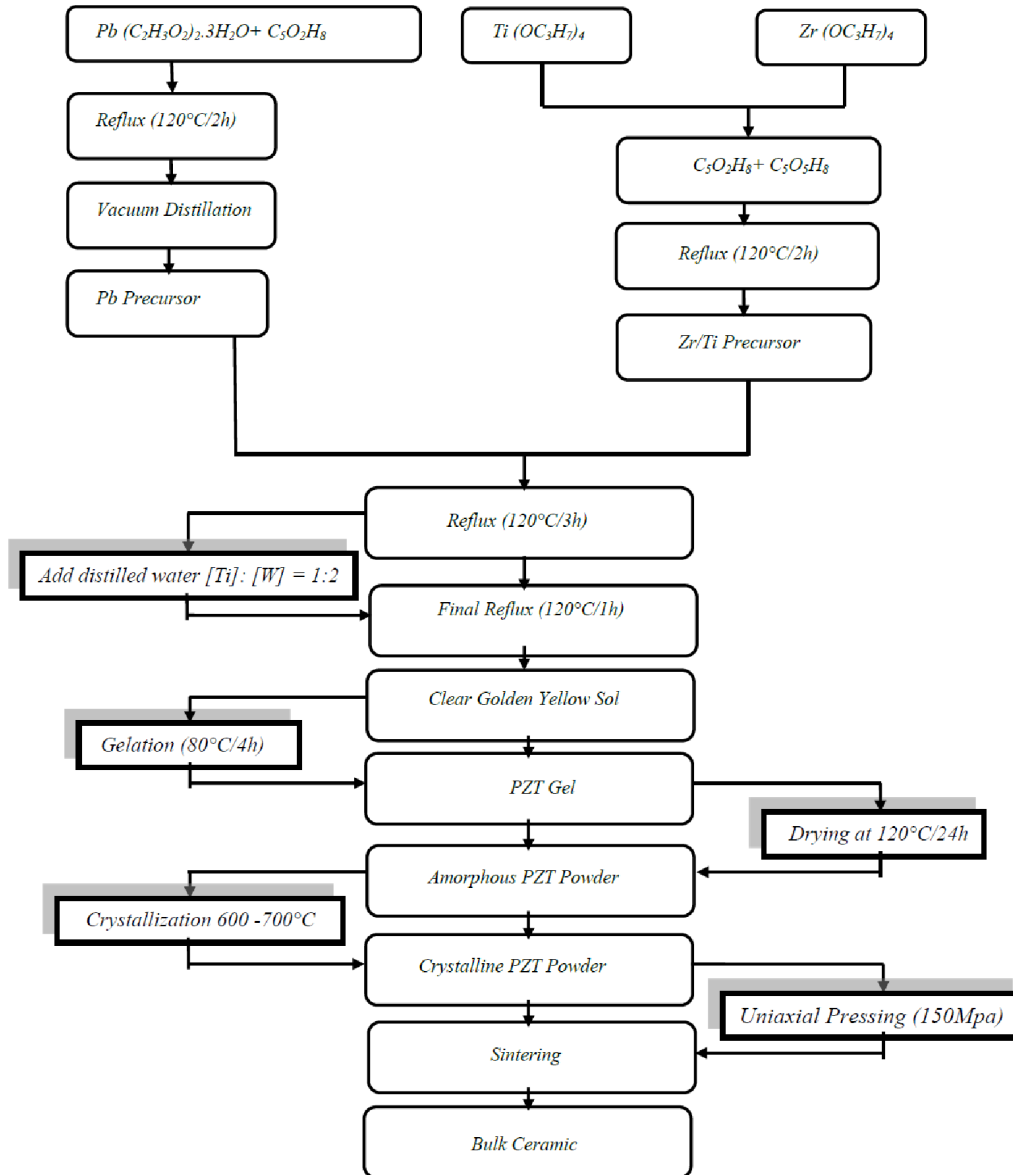


Figure 2. Preparation of PZT nanocrystalline powders and bulk PZT ceramics

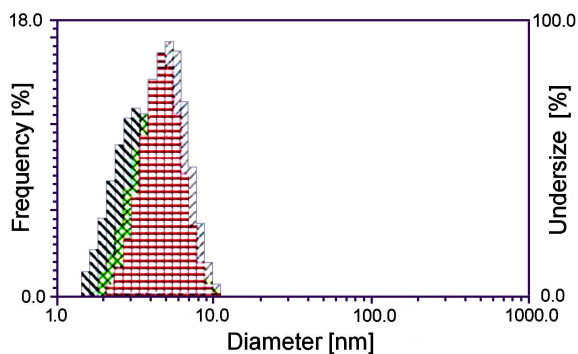


Figure 3. Particle size distribution of 0.5 M PZT powder (results of three consecutive measurements)

formed with a JEOL JEM 2010 electron microscope (LaB₆ electron gun), (JEOL, Tokyo, Japan) operating at 200 kV and equipped with a Gatan 794 Multi-Scan CCD

camera. Particle size distribution was measured using a laser particle size analyser (Horiba, LB-550), this was achieved by taking a small amounts of the powder in water and left in an ultrasonic bath before measurements. The molecular structures of the as-dried and calcined powders were studied by using a Fourier transform infrared spectrometer (FTIR-8300 Shimadzu), with a frequency ranging from 400–4000 cm⁻¹, in a KBr wafer.

III. Results and discussion

3.1. PZT sol

Figure 3 shows particle size distribution of ultrafine particles in the PZT sol. As it can be seen, nanoparticles have a diameter below 10 nm and average particle size is 5.5 nm. Figure 4 shows FTIR spectra of the PZT sols. Figure 4a shows spectrum of the PZT sol with distillation process in the final step, whereas Fig. 4b shows

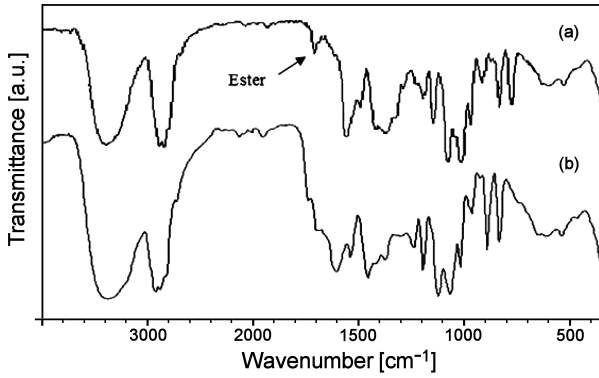


Figure 4. FTIR spectra of PZT sol without (a) and with (b) distillation process in final stage

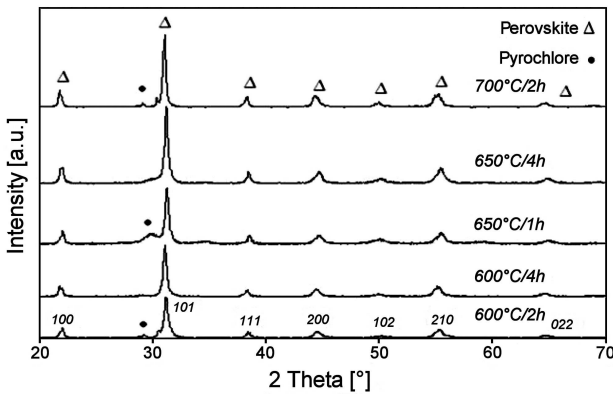


Figure 5. X-ray diffraction patterns of calcined PZT powders at various temperatures

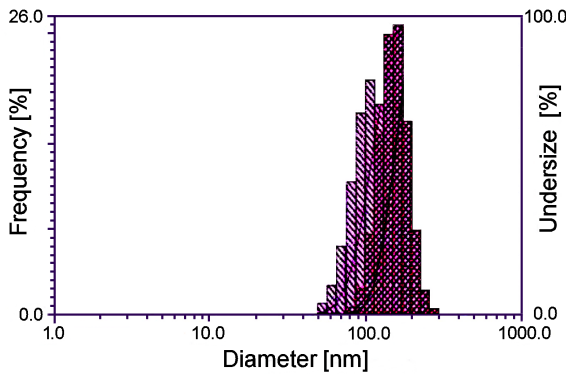
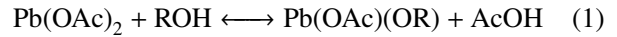


Figure 6. Particle size distribution of PZT powders calcined at 600°C/4 h (results of two consecutive measurements)

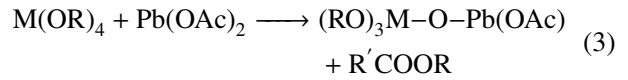
FTIR spectrum for the sol without distillation process in the final step. As it is clearly observed, the only difference between these two sols is presence of a peak located at 1739.5 cm^{-1} in the sol without distillation process in the final step. This peak is due to presence of ester with general formula of $\text{R}'\text{COOR}$, where R and R' are organic groups. During preparation of Pb solution,

ester can be formed according to these reactions:



where R is $-\text{CH}_2\text{OCH}_2\text{CH}_3$ and Ac is CH_3CO .

Ester can also be produced as a result of reaction between titanium isopropoxide or zirconium n-propoxide with lead acetate [24]:



where M is Ti or Zr, R is CH_3O and R' is CH_3 .

The presence of ester in the sols modified their properties. Thus, in order to eliminate this product (ester), distillation process must be done in the final step (Fig. 4b).

3.2. PZT powders

X-ray diffraction studies

During gel to ceramic conversion in the sol-gel derived PZT powders two crystalline phases were observed. The first one is a stable and desired phase with excellent electrical properties, i.e. perovskite phase with general formula ABO_3 ($\text{Pb}(\text{Zr}_{1-x}\text{Ti}_x)\text{O}_3$). The second one is a metastable and undesired phase, i.e. pyrochlore phase with poor electrical properties due to large defect density as a result of oxygen or lead deficiency [6], with general formula $\text{A}_2\text{B}_2\text{O}_{7-x}$ ($\text{Pb}_2(\text{Zr}_{1-x}\text{Ti}_x)_2\text{O}_{7-x}$) [25]. Therefore it is essential to avoid formation of pyrochlore phase during crystallization process. X-ray diffraction patterns of the PZT powders calcined at different temperatures with a heating rate of $5^\circ\text{C}/\text{min}$ are shown in Fig. 5. The as-dried PZT powders have an amorphous structure so XRD pattern of this powders are not shown here.

A comparison between the powders calcined at different holding time but same crystallization temperature, i.e. 600°C for 2 and 4 h, shows that prolonged heating increases amount of perovskite phase. It can be explained by the fact that pyrochlore phase is transformed to perovskite phase in a slow kinetic process [25]. The observed pyrochlore peak in XRD pattern of the powders crystallized at 650°C for 1 h, is due to insufficient holding time for complete transformation of pyrochlore to perovskite phase. So it is necessary to prolong heating for obtaining of a pure perovskite phase. Another comparison between the powders calcined at different temperatures but same holding time, i.e. 600°C and 700°C

Table 1. Relative amount of perovskite phase (P_{per}) and crystalline size of calcined PZT powders

Sintering conditions	600°C/2 h	600°C/4 h	650°C/1 h	650°C/4 h	700°C/2 h
P_{per} [%]	95	~100	93	100	97
Crystallite size [nm]	63	67	64	70	68

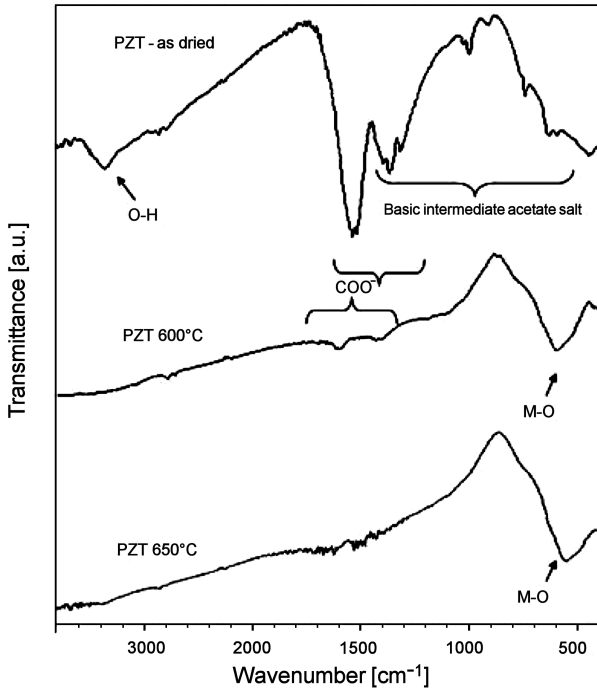


Figure 7. FTIR spectra of as-dried and calcined PZT powders at indicated temperatures for 4 h

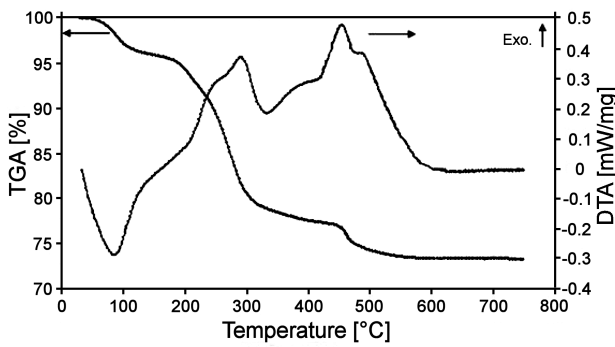


Figure 8. DTA/TGA curves of PZT gel

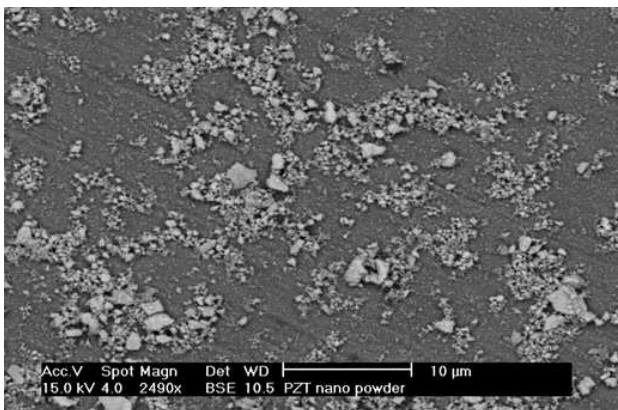


Figure 9. SEM micrograph of PZT powders after calcination at 600°C/4 h

for 2 h, shows that increase of crystallization temperature have led to increase of amount of perovskite phase and also increase of peaks intensity, which is due to better crystallinity and grain growth [25].

Average of crystalline size and amount of perovskite phase of the calcined PZT powders are shown in Table 1. Average of crystalline size was calculated using Scherrer-Warren equation:

$$x = \frac{C \cdot \lambda}{\beta \cdot \cos \theta} \quad (4)$$

where x is crystal size in angstrom, C is a numerical constant (~ 0.9), λ is the wavelength (1.5418 \AA), β is full width at half maximum (FWHM) of the XRD (110) peak in radians and θ is Bragg angle for the peak in degrees. Fraction of perovskite phase (P_{per}) was calculated approximately, for comparative purposes, from the XRD intensity peaks using the following expression [31]:

$$P_{per} = \frac{I_{110(\text{perovskite})}}{I_{110(\text{perovskite})} + I_{110(\text{pyrochlore})}} \cdot 100 \quad (5)$$

Based on the results presented in Table 1, the powders calcined at 600 °C for 4 h were selected for further sintering studies.

Particle size studies

Figure 6 shows particle size distribution of the PZT calcined at 600 °C for 4 h. A salient feature of these powders is that they have a narrow distribution and mean particle size were approximately 100 nm, indicating of formation of nanosized powders.

Fourier transformed infrared studies

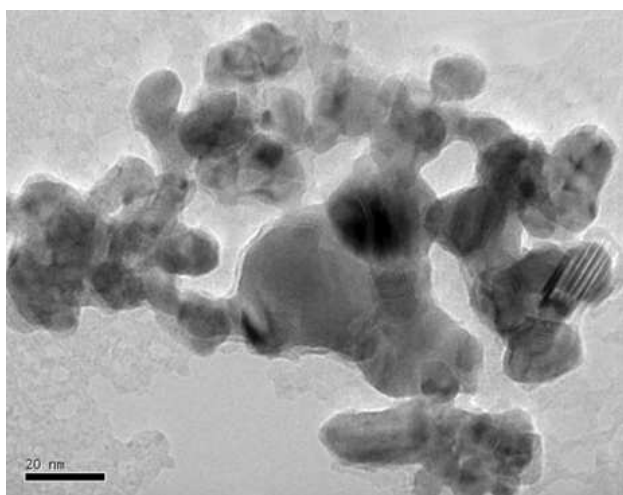
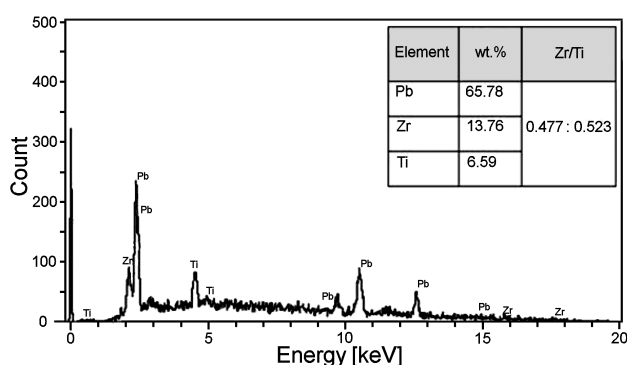
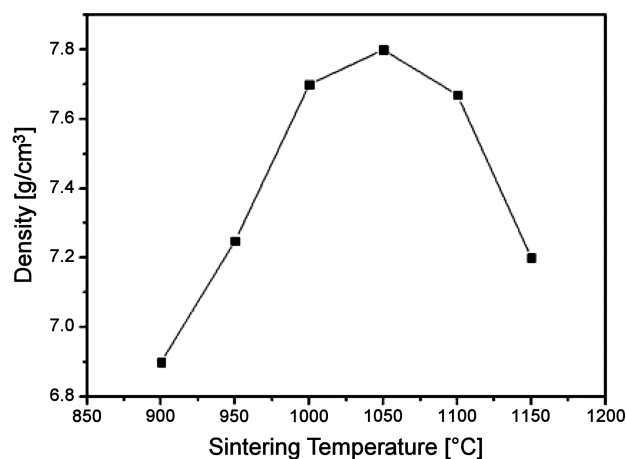
Figure 7 shows the FTIR spectrum of the as-dried and calcined powders. The as-dried powders have several peaks that are disappearing after heat treatment at higher temperatures. Also at higher temperatures a new peak is observed. The absorption band at 3444.6 cm^{-1} may be assigned to the stretching of –OH groups present in 2-methoxyethanol, acetylacetone or chemically combined water in $\text{Pb}(\text{C}_2\text{O}_2\text{H}_7)_2 \times 3 \text{ H}_2\text{O}$ [32]. The bands between 1439.9 cm^{-1} and 1623.9 cm^{-1} corresponds to the symmetric and antisymmetric –COO– stretching modes of the acetate groups [26]. These peaks are very weak at high temperatures and finally completely disappear. The peaks between 600 to 1338.5 cm^{-1} may be assigned to the carbonate presents in the as-dried powders that corresponds to the stretching mode of C–C bands and vibration modes of CH_3 groups (basic intermediate acetate salts) [26,27]. The presence of carbonaceous species in the as-dried particles is also confirmed by black colour of the powders. A sharp band at 582.5 cm^{-1} was formed in the powders calcined at 600 °C and 650 °C, that were attributed to the M–O bonding ($M = \text{Ti, Zr and Pb}$).

TGA/DTA studies

The TGA curve (Fig. 8) shows a weight loss of about 27 wt.% in the temperature range of 25–600 °C where mass loss occurs in three steps. The decomposition of

Table 2. A comparison between calcination temperature and time in this study with other papers

Crystallization temperature [°C]	Crystallization time [h]	Ref.
600	4	Present work
900	4	[29]
700	12	[30]
700	4	[31]
650	2	[9]

**Figure 10. TEM image of PZT powders calcined at 600°C/4 h****Figure 11. EDX analysis of PZT powders****Figure 12. Density variations of PZT discs as a function of sintering temperature**

the PZT gel is characterized by one endothermic peak at 100 °C due to the evaporation of physically absorbed water, solvent and volatile esters and two main exothermic peaks. Two exothermic peaks in the range of 200–300 °C are attributed to the decomposition of organic species accompanied by a large weight loss. The last two exothermic peaks are assigned to the formation of pyrochlore and of perovskite phases. There is a small weight loss along with these peaks indicating that both phenomena were accompanied by the residual combustion of the organic species. TGA/DTA and FTIR results in conjunction with XRD results show that the complete formation temperature of the perovskite PZT is 600 °C. Table 2 presents a comparison between calcination temperature and time in this study with some other researchers.

SEM/TEM and EDX analysis

The PZT powders calcined at 600 °C for 4 h were further analysed by SEM/TEM and EDX analysis. Figure 9 shows SEM micrograph of the PZT powders indicating presence of some agglomeration. Figure 10 shows TEM micrograph of these powders confirming presence of particles with irregular shape and particle sizes smaller than 100 nm.

Figure 11 presents EDX result of the PZT powder prepared by sol-gel process showing relative quantity of principal elements of PZT, i.e. Pb, Zr and Ti. It can be observed that there is no impurity in synthesized powders demonstrating high purity of starting materials and reliability of sol-gel process. Furthermore, calculated Zr/Ti ratio was 0.523/0.477 which is very close to MPB (52.3/47.7). This shows another advantage of sol-gel process, i.e. possibility exact control of stoichiometry.

3.3. PZT ceramics

Figure 12 shows effect of sintering temperature on density of the PZT ceramics. It can be observed that density increases from 6.9 g/cm³ up to 7.8 g/cm³ with increase of sintering temperature from 900 to 1050 °C. A further increase of temperature over 1050 °C caused the drop of density to 7.2 g/cm³ at 1150 °C. This variation of density with temperatures can be explained by the fact that at low temperatures, such as 900 and 950 °C, sintering is incomplete since diffusion is a thermally activated process, so density is low. Decrease of density at high temperatures is probably due to volatilization of lead and grain growth caused by high temperatures [28]. Figure 13 shows the SEM micrographs of fractured surfaces of the PZT ceramics sintered at various temperatures. It can be seen from Fig. 13a that the PZT powders sintered at 950 °C have porous structure because of incomplete sintering. At 1000 °C grain size was approximately 2 μm and sintering was not fully completed (Fig. 13b). Density of 7.8 g/cm³, very close to the theoretical density of 7.9 g/cm³, with similar grain size was achieved at 1050 °C (Fig. 13c).

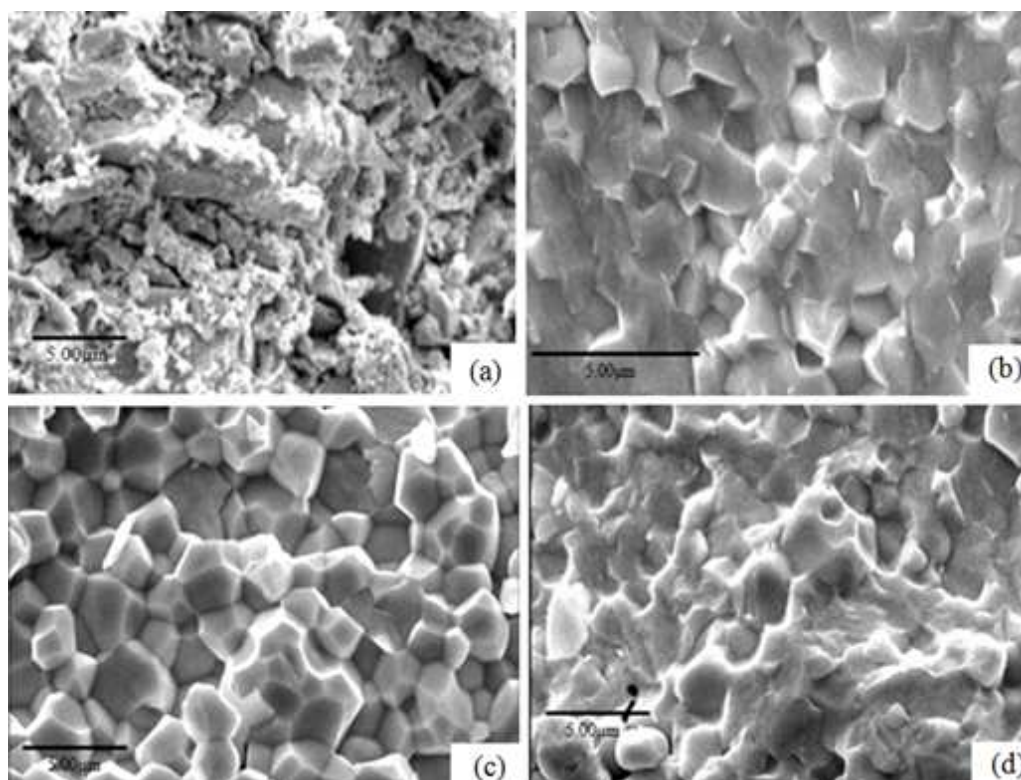


Figure 13. SEM micrographs of sintered PZT discs for 2 h at: a) 950 °C, b) 1000 °C, c) 1050 °C and d) 1100 °C

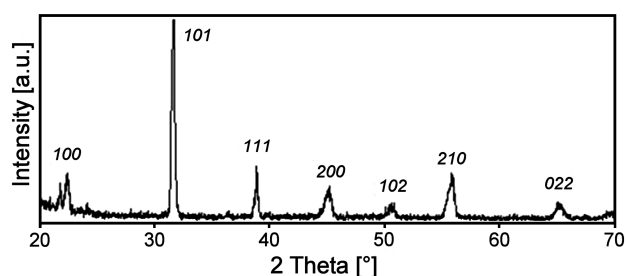


Figure 14. XRD pattern of PZT disc sintered at 1050 °C/2h

At higher temperature lead volatilization caused appearance of porosities and hence a drop in density (Fig. 13d). From the density results and SEM micrographs, it can be deduced that optimum sintering condition for the PZT discs is 1050 °C for 2 h. With sintering at such condition the pure PZT ceramics without presence of any impurity or pyrochlore phase and relative density of 98% can be obtained (Fig. 14).

IV. Conclusions

In this study nanocrystalline PZT powders (0.523/0.477) were successfully synthesized by sol-gel process. The PZT powders were completely crystallized at relatively low temperature, i.e. 600 °C. The calcined powders were sintered at various temperatures for 2 h, and the optimum sintering condition was found to be 1050 °C for 2 h. The sintered PZT ceramics have single phase perovskite structure and relative density of approximately 7.8 g/cm³, which is about 98% of their theoretical density.

Acknowledgements: Partial support of the Iran Nanotechnology Initiative Council is gratefully acknowledged.

References

1. B. Jaffe, W.R. Cook, B. Jaffe, *Piezoelectric ceramics*, Academic Press, New York, USA, 1971.
2. B. Jaffe, R.S. Roth, S. Marzullo "Piezoelectric properties of lead zirconate titanate solid-solution ceramics", *J. Appl. Phys.*, **25** (1954) 809–810.
3. D.J. Jones, S.E. Prasad, J.B. Wallace, "Piezoelectric materials and their applications", *Key Eng. Mater.*, **122-124** (1996) 71–144.
4. G.H. Heartling, "Ferroelectric ceramics: history and technology", *J. Am. Ceram. Soc.*, **82** (1999) 797–818.
5. C. Snagsubun, A. Watcharapasorn, M. Naksata, T. Tunkasin, S. Jiansirisomboon, "Preparation of sol-bonded lead zirconate titanate ceramics via sol-gel and mixed-oxidized methods", *Ferroelectrics*, **356** (2007) 197–202.
6. R. Tahar, N. Tahar, A. Salah, "Preparation and characterization of PZT solid solutions via sol-gel process", *J. Cryst. Growth*, **307** (2007) 40–43.
7. R.F. Zhang, L.B. Kong, Y.Z. Chen, T.S. Zhang, "PZT ceramics derived from hybrid method of sol-gel and solid-state reaction", *Mater. Lett.*, **55** (2002) 388–393.
8. M.N. Rahaman, *Ceramic Processing and Sintering*, 2nd ed., Marcel Dekker, New York, USA, 2003.
9. Z.D. Qing, W. Jun, S. Shang, W. Li, C. Sheng, "Synthesis and mechanism research of an ethylene glycol-

- based sol-gel method for preparing PZT nanopowders”, *J. Sol-Gel Sci. Technol.*, **41** (2007) 157–161.
10. S. Linardos, Q. Zhang, J.R. Alcock, “An investigation of the parameters effecting the size of a PZT ceramic powder prepared with a sol-gel technique”, *J. Eur. Ceram. Soc.*, **27** (2007) 231–235.
 11. C. Liu, B. Zou, A.J. Rondinone, Z.J. Zhang, “Sol-gel synthesis of free-standing ferroelectric lead zirconate titanate nanoparticles”, *J. Am. Ceram. Soc.*, **123** (2001) 4344–4345.
 12. A. Banerjee, S. Bose, “Free-standing lead zirconate titanate nanoparticles: low-temperature synthesis and densification”, *Chem. Mater.*, **16** (2004) 5610–5615.
 13. B. Su, T.W. Button, C.B. Ponton, “Control of the particle size and morphology of hydrothermally synthesized lead zirconate titanate powders”, *J. Mater. Sci.*, **39** (2004) 6439–6447.
 14. R. Lal, R. Krishnan, P. Ramakrishnan, “Preparation and characterization of submicron reactive PZT powders”, *Mater. Sci. Eng.*, **96** (1987) L25–L29.
 15. K.R. Rao, A.V. Rao, S. Komarneni, “Preparation PZT precursor powder by co-precipitation”, *Mater. Lett.*, **28** (1996) 463–467.
 16. Q. Meng, K. Zhu, X. Pang, J. Qiu, B. Shao, H. Ji, “Sol-hydrothermal synthesis and characterization of lead zirconate titanate fine particles”, *Adv. Powder Technol.*, **24** (2013) 212–217.
 17. J. Livage, M. Henry, C. Sanchez, “Sol-gel chemistry of transition metal oxides”, *Prog. Solid State Chem.*, **18** (1988) 259–341.
 18. C.J. Brinker, G.W. Scherer, *Sol-Gel Science*, Academic Press, New York, USA, 1990.
 19. A.S. Gomeza, R. Sato-Berrú, R.A. Toscano, J.M.S. Blesa, C. Pinar, “On the synthesis and crystallization process of nanocrystalline PZT powders obtained by a hybrid sol-gel alkoxides route”, *J. Alloys Compd.*, **450** (2008) 380–386.
 20. R. Thomas, S. Mochizuki, T. Mihara, T. Ishida “Preparation of ferroelectric $\text{Pb}(\text{Zr}_{0.5}\text{Ti}_{0.5})\text{O}_3$ thin films by sol-gel process: dielectric and ferroelectric properties”, *Mater. Lett.*, **57** (2003) 2007–2014.
 21. M. Zhang, I.M. Salvado, P.M. Vilarinho, “Synthesis and characterization of lead zirconate titanate fibers prepared by the sol-gel method: the role of the acid”, *J. Am. Chem. Soc.*, **86** (2003) 775–781.
 22. C. Galassi, “Processing of porous ceramics: Piezoelectric materials”, *J. Eur. Ceram. Soc.*, **26** (2006) 2951–2958.
 23. S. Li, R.A. Condrate Sr., R.H. Spriggs, “A FTIR and Raman spectral study of the preparation of lead titanate (PbTiO_3) by sol-gel method”, *Spectrosc. Lett.*, **21** [9-10] (1988) 969-980.
 24. J. Livage, C. Sanchez, “Sol-gel chemistry”, *J. Non-Cryst. Solids*, **145** (1992) 11–19.
 25. R. Tahar, N. Tahar, A. Salah, “Low temperature Processing and characterization of single-phase PZT powders by sol-gel method”, *J. Mater. Sci.*, **42** (2007) 9801–9806.
 26. T.I. Chang, J.L. Huang, H.P. Lin, S.C. Wang, H.H. Lu, L. Wu, J.F. Lin, “Effect of drying temperature on structure, phase formation, sol-gel derived lead zirconate titanate powders”, *J. Alloys Compd.*, **414** (2006) 224–229.
 27. Y. Faheem, M. Shoaib, “Sol-gel processing and characterization of phase-pure lead zirconate titanate nano-powders”, *J. Am. Ceram. Soc.*, **89** (2006) 2034–2037.
 28. C. Sangsubun, A. Watcharapasorn, T.S. Jiansirisomboon, “Densification and microstructure of lead zirconate titanate ceramics fabricated from a triol sol-gel powder”, *Curr. Appl. Phys.*, **8** (2008) 61–65.
 29. C.L. Huang, B.H. Chen, L. Wu, “Application feasibility of $\text{Pb}(\text{Zr,Ti})\text{O}_3$ ceramics fabricated from sol-gel derived powders using titanium and zirconium alkoxides”, *Mater. Res. Bull.*, **39** (2004) 523–532.
 30. C. Liu, B. Zou, A.J. Rondinone, Z.J. Zhang, “Sol-gel synthesis of free-standing ferroelectric lead zirconate titanate nanoparticles”, *J. Am. Chem. Soc.*, **123** (2001) 4344–4345.
 31. T.K. Mandal, S. Ram, “Synthesis of $\text{PbZr}_{0.7}\text{Ti}_{0.3}\text{O}_3$ nanoparticles in a new tetragonal crystal structure with a polymer precursor”, *Mater. Lett.*, **57** (2003) 2432–2442.